NUMERICAL STUDY OF THE MICROCHANNEL WITH A COMPOSITE STRUCTURE OF CIRCULAR TUBE RIBBED AND WAVY RUNNER

Xuanyou CHEN [1,*]

Based on the straight microchannel with circular section, three different structural models are designed in this paper, which are circular tube wave channel, ribbed wave channel and ribbed direct current channel. The laminar heat transfer state was numerically studied. The results show that, under the same thermal load, the overall thermal resistance can be reduced by adding inner ribs to the circular tube microchannel, and the pressure drop can be increased sharply to improve the heat transfer efficiency. Based on the linear microchannels with circular cross-section, three different structural models are designed in this paper, namely, circular tube wave channel, ribbed wave channel and ribbed DC channel. The laminar flow heat transfer state was investigated numerically. The results show that the total thermal resistance can be reduced by adding internal ribs to the circular tube microchannel under the same thermal load, while the pressure drop can be increased significantly to improve the heat transfer efficiency. The simulation results show that the average temperature and temperature difference of the heat sink can be reduced by 42°C and 28°C, respectively, in the composite structure of ribs and wavy flow channels compared with the circular straight tube microchannels. The heat dissipation performance is most obvious when Re<300 with increasing flow velocity. At relatively low Reynolds number, the composite structure of rib and wave runners can increase the heat dissipation characteristics of the microchannel. In addition, the period and amplitude of the waves may have different impacts on the thermal perfomance for the same flow resistance.

Keywords: circular tube microchannel; electronic chip; micro-scale heat transfer; laminar flow in tubes; fluid-solid coupling numerical simulation

[1] Jiangsu University of Science and Technology; Jiangsu Province, China, email: 526748614@qq.com

1. Introduction

Due to rapid evolution in Integrated circuits, the concept of heat management has been widely introduced into the industry. Several traditional heat dissipation technologies cannot meet the demands of the ever-increase cooling for electronic devices, and the heat dissipation issues of device plays a crucial role in the further development of advanced electronic products. Khan[1] et al. studied the heat transfer efficiency of two conventional tubular heat sinks (circular and elliptical) and a circular microchannel heat sinks. It is found that the microchannel heat sink has higher heat transfer efficiency than the two conventional heat exchangers. Lei Cai [2] et al. designed eccentric ribs with five different shapes, such as rectangle, rear triangle, isosceles triangle, front triangle and semicircle. It is found that the enhanced heat transfer effect of eccentric ribs are significant with larger pressure drop. When Re<350, the performance evaluation index of the front triangular rib microchannel radiator is the highest, and the performance evaluation index of the rectangular rib microchannel radiator is the lowest. In Re>400, the performance evaluation standard of the semicircular offset rib is the best, and the performance evaluation standard of the rear triangular offset rib is the worst. It was also found that the advantage of heat transfer enhancement by offset ribbed microchannel radiators decreases gradually at higher Reynolds numbers due to the significant pressure drop. Sakanova [3] found that the closer the introduced microstructure is to the streamline shape, the smaller the range of fluid disturbance around it. Some scholars, inspired by bionics, have designed bionic microstructures such as fish scale[4] and wing[5] whose own unique streamline shapes have good drag reduction properties. Liu[6] compared the flow characteristics and comprehensive performance of the diamond-shaped spoiler structure and found that the more the number of spoiler structures, the better the heat dissipation performance, which can be applied to the heat dissipation of electronic components. The fully developed laminar flow and heat transfer in periodic serpentine channels with different cross-sectional shapes were studied numerically by Fletcher [7-12] et al. The results show that the outlet pressure drop of the three hybrid modules is in the order for circular, trapezoidal and rectangular modules from high to low under the same flow conditions. Conventional microchannel heat sinks usually use linear channels with almost straight flow lines of refrigerant, thus poor mixing of hot and cold fluids and low heat transfer efficiency. Y.Sui. [13] found that when the coolant flows through the wavy microchannel, a secondary flow is generated. The presence of secondary flow enhances fluid perturbation, and thus improves mixed heat

transfer. Many researchers have applied this mechanism in intensive heat transfer efficiency. [14-17] Xie et al.[18] proposed a transverse wavy microchannel based on a linear microchannel with a rectangular cross-section. The overall thermal performance of the transverse wavy microchannel is superior to that of the conventional right-angle rectangular microchannel. Gongnan Xie et al. [19] designed a longitudinal microchannel and a transverse microchannel, respectively, and found that when considering the geometry, the overall thermal performance of longitudinal microchannels is lower than that of right-angle rectangular microchannels. And the transverse microchannels have a great potential to reduce the pressure drop. Lin [20]modified the design of the wave-type microchannel by varying the wavelength and amplitude of the channel , comparing the newly designed scheme with the most original wave-type channel. I was found that the thermal performance is improved, when the unit wavelength or amplitude of the wave is increased. Liang Gong[21]et al. considered two different types of wave channels by changing different wave-like characteristic amplitudes and wavelengths in the Re range from 50~150. The total thermal performance of the wavy channel was improved by comparing it with the straight channel. The optimal configuration integrity can be improved by up to 55%, and the heat transfer performance increases with increasing wave amplitude and decreasing wavelength. Manglik, Raj M. et al. [22] studied steady forced convection with a periodically developing low Re (100 ~1000) three-dimensional wavy plate fin flow core. It shows that the effect of wavy fin density on velocity, temperature distribution, Fanning friction coefficient and Colburn coefficient. The performance evaluation factor (j/f) increases with the fin density, and the heat exchange effect is more prominent. Valaparla Ranjith Kumar et al. [11] studied hydrothermal characteristics of a circular wavy microchannel with bifurcated plates and compared it with a sinusoidal wave-shape heat sink. The numerical studies were performed at Re of 100 ~ 300. It was found that the circular wavy microchannels with bifurcated plates have higher Nu and pressure drop penalties.

Based on the above enhanced heat exchange method, a hybrid microchannel structure with different flow channels and increased inner ribs will be proposed in this paper. It can be used in microelectronics cooling systems, such as computer CPU cooling. The three-dimensional data model is established and numerical simulations are used to study the flow and heat transfer performance of the hybrid module.

2. Numerical simulation

2.1 Physical model of heat sinks

Fig. 1 shows the diagram of the model structure. On the basis of circular tube, three models are designed, namely circular tube wave channel, ribbed direct current channel and ribbed wave channel. The repeatability and symmetry of the microchannel heat sink are taken into account. Therefore, in this numerical study, the cells in the microchannel are selected for simulation. Fig. 2 shows the computational domain of the microchannel, the mesh model and the main view of the microchannel cross-section geometry. L, W, H are the length, width, and height of the micro-channel. They are 20 mm, 1.0 mm and 1.0 mm, respectively. D_h is the hydraulic diameter of the channel. The structural parameters of the model is shown in table1.

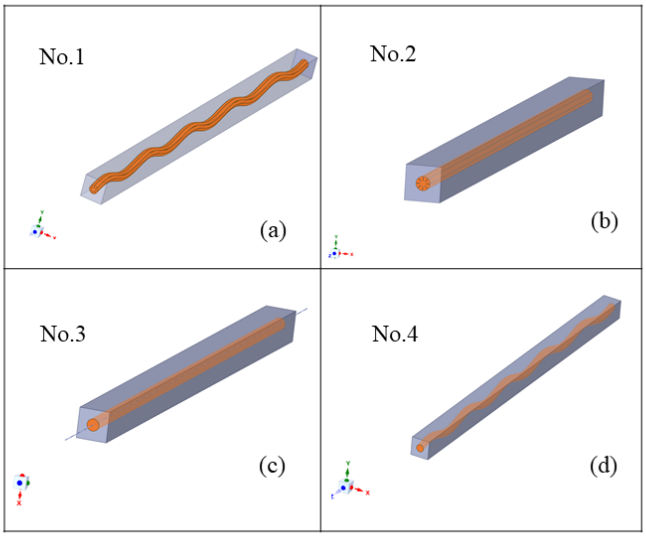

Fig 1. Four microchannel types, (a) circular wave unit with ribs; (b) circular straight unit with ribs; (c) circular straight unit; (d) circular wave unit.

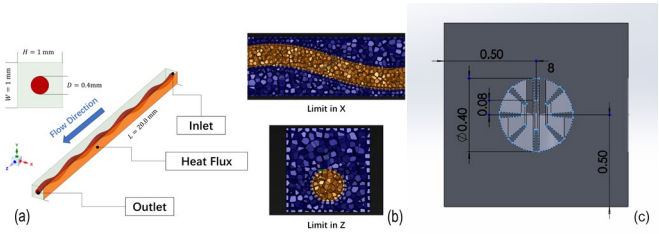

Fig 2. (a)The computational domain diagrams of heat sinks; (b) model mesh;(c) geometric parameter of heat sink (No.1 and No.2)

Table1

The geometrical parameters of four modes

Number	the length of ribs/mm	D_h/mm
No.1	0.12	0.137
No.2	0.12	0.137
No.3	-	0.4
No.4	-	0.4

2.2 Numerical model of heat sinks

The solid region material is silicon and the workpiece is water. We can make some assumptions:

(a) Incompressible, laminar and steady state.

(b) The thermophysical properties is constant.

(c) No Viscous dissipation, gravity effects and the radiation effects

Based on these assumptions, The equations for continuity, momentum, and energy conservations can be described as followings:

$$\nabla \cdot (\rho \vec{V}) = 0 \tag{1}$$

$$\nabla \vec{V} \cdot (\rho \vec{V}) = -\nabla p + \nabla(\mu \nabla \vec{V}) \tag{2}$$

$$\nabla \cdot (\rho c_p \vec{V} T_f) = \nabla \cdot (\lambda_f \nabla T_f) \tag{3}$$

For solid domain, the energy equation is obtained as followings:

$$\lambda_s \nabla^2 T_s = 0 \tag{4}$$

where $\rho, \vec{V}, p$, μ, λ_f, C_p, T_f, λ_s and T_s are the density of the fluid, the velocity vector, the pressure, viscosity, thermal conductivity, specific heat capacity of fluid, temperature of the fluid, the thermal conductivity and temperature of the solid respectively.

$$\mathrm{Re} = \frac{\rho u_{in} D_h}{\mu} \tag{5}$$

where u_{in} represents the inlet flow velocity.

The friction factor is calculated by followings:

$$f = \Delta p(\frac{2D_h}{\rho u_{in}^2}) / L \tag{6}$$

where Δp represents the pressure drop of the fluid.

$$Nu = \frac{h_m D_h}{\lambda_f} \tag{7}$$

where h_m represents the average heat transfer coefficient.

$$h_m = \frac{qA_b}{A_w(T_w - T_f)} \tag{8}$$

Where q, A_b, A_w, T_w, T_f are the heat flux, the heated area, the heat exchanger area, the average temperature of the solid and the temperature of fluid, respectively.

$$Q = qA_b \tag{9}$$

Where Q is the total heat load. Especially, A_w depends on different types of heat sinks.

The thermal resistance is written by:

$$R = \frac{T_{\max} - T_{in}}{Q} \tag{10}$$

where T_{max} represents the maximum temperature of the solid, and T_{in} is the temperature of the inlet fluid.

The initial temperature of the fluid inlet T=300K, and the ambient temperature of the solid T=300K. The heat flux applied to the heating surface of the

heat sink is q=600000 W/m^2. Using the finite element method, the simulation on the commercial software ANSYS Fluent is carried on this study.

2.3 Grid verification

To eliminate the errors due to the mesh thickness, the mesh size was independently verified before the detailed analysis. The relative error was obtained by the followings:

$$e\% = \left| \frac{J_2 - J_1}{J_1} \right| \times 100 \tag{11}$$

Where J is arbitrary parameters; such as temperature, pressure and Nusselt number, J_1 is the parameter value obtained from best grid, where J_2 is the parameter value obtained from the other grid. Table 2 displays the errors of temperature and pressure for different grids with best grid numbers of 3.799 million. It can be seen that the amount of grid number for 0.884 million has a better result. Thus, the grid of 0.884 million cells was selected in this paper.

Table 2

Grid independent test.

No.	Number of grids / ×10^6	T/K	e%	Pressure/Pa	e%
1	3.799	304.75	-	2672.84	-
2	3.074	304.56	0.06	2670.66	0.08
3	2.083	304.28	0.09	2682.77	0.45
4	1.308	304.06	0.07	2704.15	0.80
5	0.884	303.95	0.04	2721.57	0.64

3. Analysis and discussion of the results

3.1 Flow heat transfer performance parameters

The flow state is reflected by the flow velocity and flow direction, which reflect the hydraulic performance of the structure. Fig.3 displays the flow diagram of velocity contour in the flow channel of the central section of the four channel structures under the flow working medium. It shows that the velocity distribution of the straight channel structure channel is the most uniform, with the presence of fractional velocities in the non-flow direction of the wave channel. On the unbiased

rib structure, both near the boundary structural part difference, can be seen from the diagram, the smooth wave passage does not produce obvious vortexes, and the velocity increases obviously due to the existence of the side ribs, the center of the pipe has the highest flow rate.

Fig.4 displays the pressure contour in each channel and heat flow boundaries. It shows that the pressure drop at each operating condition increases, and the range of sliding friction resistance between the channel and the wall surface increases, which causing the increase of fluid flow resistance. The pressure drop in the channels with bias ribs is larger than that in the channels without bias ribs, due to the lateral bias ribs increase the resistance to fluid flow. When the water flows through the ribbed structure, the pressure decreases with the narrowing of the channel

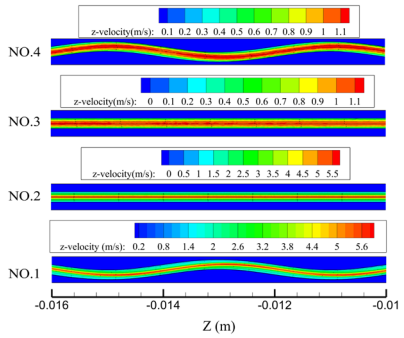

Fig.3.The contour of velocity and streamline of four heat sinks (x=-0.03615m) at Re=300

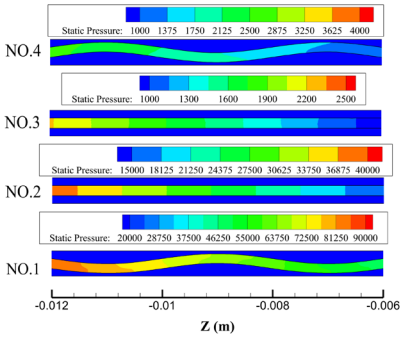

Fig.4. The contour of pressure for four heat sinks (x=-0.03615m) at Re=300

The microchannels with ribs can effect the heat exchanger performance. The temperature distribution of the microchannels is shown in Fig. 5. It can be seen that the temperatures of microchannels No.3 and No.4 are much higher than those of the

other microchannels. And the temperature distribution of No.3 resembles a smooth linear distribution with insignificant changes in temperature gradients. As shown in Fig.5, the presence of ribs in the channel causes a significant temperature drop in No.1 and No.2.

Fig.6 the No.3 has the highest average temperature, and No. 4 is in the second place, but they are not significant. No.1 and No.2 have the best performance. While the temperature difference and the average temperature of the models with ribbed structures (No.1 and No.2) vary drastically until Re =300, and then the rate of change decreases slowly. This shows that this method of reducing the temperature of the heat sink by increasing the fluid velocity is not always effective. At Re=150, the average temperature and temperature difference of No.1 decreased by 42°C and 28°C, respectively.

Fig. 7 and Fig. 8 show the changes of pressure drop (Δp) and flow friction factor (*f*) of Re= 150 ~ 750, respectively. Δp showed a continuous and rapidly increase with the increase of Re in the partial ribbed structure (No.1 and No.2), and was significantly higher than that in the structure without ribs. In addition, the wavy channel resulted in different rates of pressure drop increase, with No.1 microchannel having the highest rate. The friction factor (*f*) decreases, and the change trend of the four models is basically the same, among which No.2 is relatively the smallest.

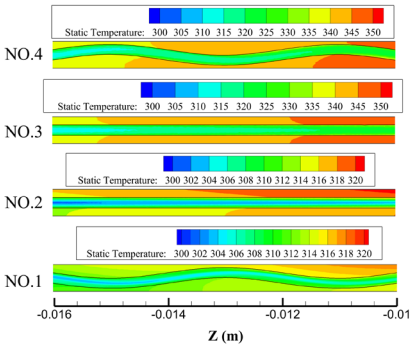

Fig.5. The contour of temperature for four heat sinks (x=-0.03615m) at Re=300

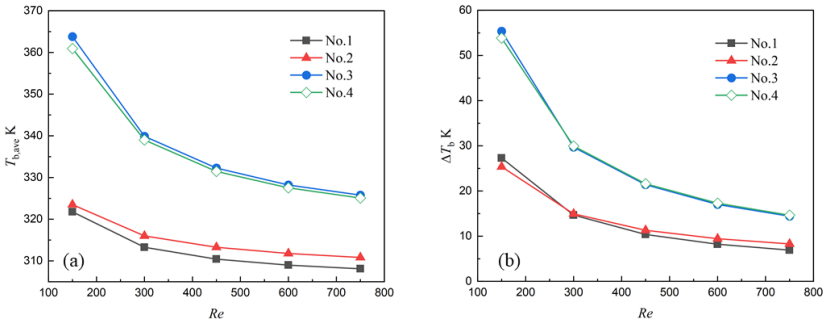

Fig.6 The decrease of the average temperature and temperature difference on the heated surface

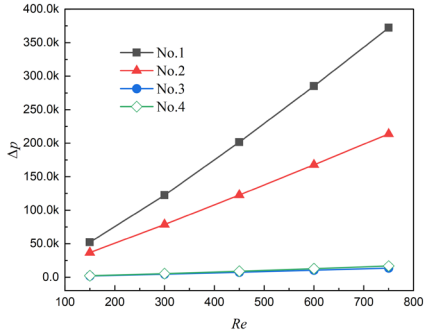

Fig.7. The comparison of pressure drop

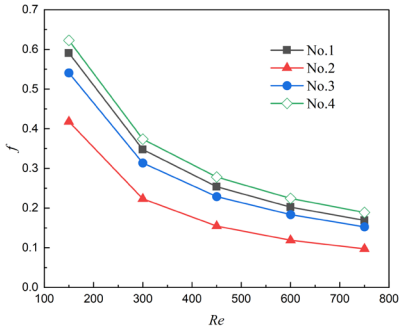

Fig.8. The decrease of friction factor

Fig.9 displays the thermal resistance of the structure with ribs is significantly lower than that of the structure without ribs, while the thermal resistance of the wave channel does not vary much compared to that of the DC channel, which may be related to the periodicity and amplitude of the structure. The thermal resistance of the four models are all reduced, and the trend of change is most visible when Re is between 150 and 300. Fig. 10 shows that the Nu increases with Re, and the rate of increase reduces after Re=450. For No.1 and No.2, heat transfer area increased, but Nu decreased significantly. The Nu of No.1 is greater than that of No.2.

The flow heat transfer enhancement mechanism regarding microchannel No.1 can be described as followings: (1) the convection area increases due to the waves and ribs, resulting in enhanced thermal performance. (2) the flow path of the wave channel is longer, which indirectly increases the heat exchanger area surface. Consequently, thermal performance is improved. For the same microchannel, the

higher the velocity is, the higher the relative Nusselt number will be. The reason is that the high-speed fluid can take away the shunt body inside the microchannel (No.1) to avoid the fluid staying in the groove of the partial ribbed structure. Thus it makes the boundary layer thinner and enhances the intensity of heat transfer. (3) When at low Re, the ribs effectively enhances the perturbation influence on the core flow domain. This conclusion has been verified [23](4) when the fluid flows into the wave channel with ribs, its radial flow is stronger than the flow in the micro-channel without ribs. This combination of wave channels and ribs results in better mixing of the fluid, forming chaotic advection, which can enhance heat transfer performance.

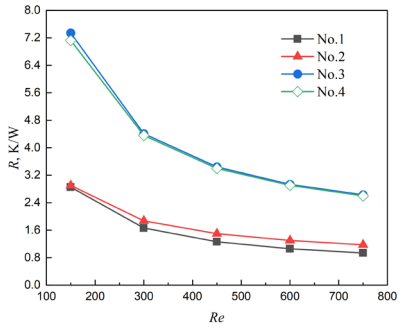

Fig.9. The comparison of the overall thermal resistance

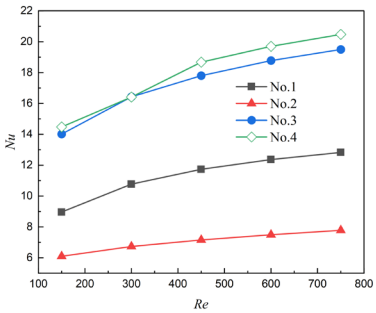

Fig.10. The Nusselt number (*Nu*) of four heat sinks

3.2 Performance evaluation

Performance evaluation criteria (*PEC*) can be comprehensively analyze the strength of the flowing heat transfer effect of microchannels. It is calculated as

$$PEC = \frac{Nu / Nu_0}{(f / f_0)^{1/3}} \tag{12}$$

Fig.11 displays the influence of three new microchannels on enhancing heat transfer coefficient at different velocities. The enhanced heat transfer coefficient tends to increase with Re. The enhanced heat transfer coefficient of the structure with biased ribs is larger than that of the structure without biased ribs. Therefore, the bias-ribbed characteristic structure can significantly enhance the comprehensive performance of the microchannels.

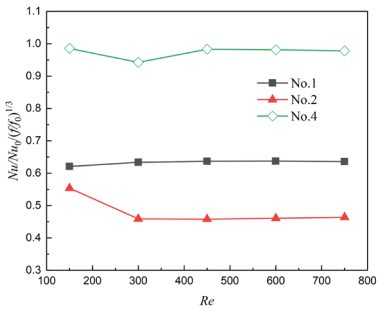

Fig.11. Variation of $Nu/Nu_0/(f/f_0)^{1/3}$with Re

3.3 Analysis of the entropy production mechanism of microchannels

Entropy production is caused by the inevitable irreversibility of the actual thermal process. The entropy yield mechanism is invoked in this study, for analyzing the flowing and heat transfer irreversibility of microchannels with four type models. The entropy production rate consists of: (1) the entropy production rate caused by the flow friction when the fluid flows through the channels ($\dot{S}'''_{gen,\Delta p}$); (2) the entropy production rate caused by the temperature difference between the fluid and the inner wall ($\dot{S}'''_{gen,\Delta T}$). And the total entropy production rate ($\dot{S}'''_{gen}$) is given by [24]:

$$\dot{S}'''_{gen,\Delta p}=\frac{\mu}{T_{\mathrm{f}}}\{2[(\frac{\partial u}{\partial x})^2+(\frac{\partial v}{\partial y})^2(\frac{\partial w}{\partial z})^2]+(\frac{\partial u}{\partial y}+\frac{\partial v}{\partial x})^2+(\frac{\partial u}{\partial z}+\frac{\partial w}{\partial x})^2(\frac{\partial v}{\partial z}+\frac{\partial w}{\partial y})^2\} \tag{13}$$

$$\dot{S}'''_{gen,\Delta T}=\frac{\lambda_{\mathrm{f}}}{T_{\mathrm{f}}{}^2}[(\frac{\partial T}{\partial x})^2+(\frac{\partial T}{\partial y})^2(\frac{\partial T}{\partial z})^2] \tag{14}$$

$$\dot{S}'''_{gen}=\dot{S}'''_{gen,\Delta \mathrm{p}}+\dot{S}'''_{gen,\Delta T} \tag{15}$$

By integrating Eqs.[25, 26] ,it can be calculated:

$$\dot{S}_{gen,\Delta \mathrm{p}}=\iiint_{\Omega}\dot{S}'''_{gen,\Delta \mathrm{p}}dV=\frac{\dot{m}}{\rho T_f}\Delta p \tag{16}$$

$$\dot{S}_{gen} = \dot{S}_{gen,\Delta \mathrm{p}} + \dot{S}_{gen,\Delta \mathrm{T}} = \frac{\dot{m}}{\rho T_f} \Delta p + \frac{q A_b (T_w - T_f)}{T_f T_w} \quad (17)$$

$$\dot{S}_{gen,\Delta \mathrm{T}} = \iiint_{\Omega} \dot{S}'''_{gen,\Delta T} dV = \frac{Q(T_w - T_f)}{T_f T_w} = \frac{q A_b (T_w - T_f)}{T_f T_w} \quad (18)$$

where $\dot{m}$ is the mass flow rate, and V is the volume of fluid.

In order to visually analyze the differences the irreversibility of the novel heat sink and the reference channel, the entropy production number can be calculated:

$$N_{s,a} = \dot{S}_{gen} / \dot{S}_{gen,0} \quad (19)$$

where $\dot{S}_{gen,0}$ is the overall entropy production of the reference heat sink (model No.3). If the value of $N_{\mathrm{s,a}}$ of the enhanced microchannel structure (No.1) is less than 1, the enhanced microchannel can decrease the irreversibility of fluid flow and heat transfer. Therefore, according to the second law of thermodynamics, the enhanced micro-channel has better thermal performance.

Fig.12(a) and (b) show that the entropy production rate caused by the flow friction has significant improvement, especially in the No. 1 and No. 2 channels. The high pressure drop leads to a significant improvement in the entropy production rate caused by flow. The value $\dot{S}_{gen,\Delta \mathrm{T}}$ reduces as increasing Re. Among the four models, No.1 has the lowest value $\dot{S}_{gen,\Delta \mathrm{T}}$, which indicates that the ribs can decrease the gradient of temperature field.

Fig. 13 displays that the value of $N_{\mathrm{s,a}}$ of No. 1 is the lowest. In the new heat sink, the compounding effects of the corrugated channels and ribs reduces the temperature gradient of the fluid. It also reduces the heat exchange irreversibility of the heat sinks, but increases heat transfer efficiency. Fig. 5 and Fig. 10 proved that the No.1 channel has a combination of more uniform temperature distribution, higher thermal performance and less irreversibility.

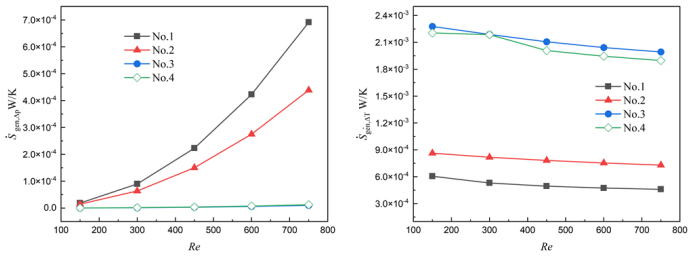

Fig.12.The entropy production rate caused by flow loss (a) and heat exchange (b) of four micro-channels.

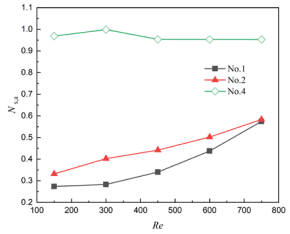

Fig.13 Ratio of the number of accretion entropy production for three new micro-channels

4.Conclusion

Three new micro-channel heat sinks are designed in this study, which consists of the combination of ribs and corrugated channels. The following conclusions can be obtained from this simulation.

(1) The pressure drop of the heat sinks with ribbed structure increases significantly. Among the four structures, Wavy structure and ribbed structure have the greatest pressure drop loss. The ribbed structure of the microchannel heat exchanger is more effective in the lower Reynolds number flow condition

(2) The ribs structure can strengthen fluid disturbance in the channels, and then enhancing the convective heat transfer. It can increase the heat exchange area and the heat transfer per unit time under certain conditions.

(3) Compared with the circular linear microchannel, the average temperature and temperature difference of the micro-channels' heating surface with ribbed and wavy runner composite structure were reduced by 42°C and 28°C, respectively. The heat dissipation performance is most pronounced with increasing flow rate when Re < 300. In this paper, the thermal effect was impacted by the influence of the period and amplitude of the corrugated channel, which was not as good as expected. Due to the obvious pressure drop caused by the wave bars, the resistance generated

by the wave flow channel should be taken into account for composite structures with wave bars.

REFERENCES

[1] *Khan M G, Fartaj A, Ting D S K.*, An experimental characterization of cross-flow cooling of air via an in-line elliptical tube array. International Journal of Heat and Fluid Flow, 2004, 25(4): 636-48.

[2] *Chai L, Xia G D, Wang H S.,* Numerical study of laminar flow and heat transfer in microchannel heat sink with offset ribs on sidewalls. Applied Thermal Engineering, 2016, 92: 32-41.

[3] *Sakanova A, Tseng K J.*, Comparison of pin-fin and finned shape heat sink for power electronics in future aircraft. Applied Thermal Engineering, 2018, 136: 364-74.

[4] *Dey P, Saha S K.*, Fluid flow and heat transfer in microchannel with porous bio-inspired roughness. International Journal of Thermal Sciences, 2021, 161.

[5] *Zhang T.I., Guo Z.P., Niu F.L.*, Flow heat transfer characteristics of wing-type microchannel high-efficiency compact heat exchangers. Atomic Energy Science and Technology, 2020: 7.

[6] *Liu Congrui, Ren Feixue, Huang Shankhao, Wang Xiaojie, Zhang Xingli,* Study on the flow heat transfer characteristics of microchannels by rhombic disturbed element structure_Congrui Liu. Journal of Natural Sciences, Heilongjiang University,2021.05

[7] *Rosaguti N R, Fletcher D F, Haynes B S.,* Laminar flow and heat transfer in a periodic serpentine channel with semi-circular cross-section. International Journal of Heat and Mass Transfer, 2006, 49(17-18): 2912-23.

[8] *Rosaguti N R, Fletcher D F, Haynes B S.,* Laminar Flow and Heat Transfer in a Periodic Serpentine Channel. Chemical Engineering & Technology, 2005, 28(3): 353-61.

[9] *Geyer P, Rosaguti N, Fletcher D, et al.,* Laminar thermohydraulics of square ducts following a serpentine channel path. Microfluid Nanofluid, 2006, 2(3): 195-204.

[10] *Geyer P E, Fletcher D F, Haynes B S.,* Laminar flow and heat transfer in a periodic trapezoidal channel with semi-circular cross-section. International Journal of Heat and Mass Transfer, 2007, 50(17-18): 3471-80.

[11] *Kumar V R, Balasubramanian K, Kumar K K.*, Numerical Prediction of Heat Transfer and Fluid Flow Characteristics in a Circular Microchannel with Bifurcation Plate. International Journal of Mathematical, Engineering and Management Sciences, 2019, 4(6): 1384-96.

[12] *Kumar V R, Balasubramanian K, Kumar K K, et al.*, Numerical investigation of heat transfer and fluid flow characteristics in circular wavy microchannel with tangentially branched secondary channels. Proceedings of the Institution of Mechanical Engineers, Part E: Journal of Process Mechanical Engineering, 2019, 233(6): 1304-16.

[13] *Sui Y, Teo C J, Lee P S, et al.,* Fluid flow and heat transfer in wavy microchannels. International Journal of Heat and Mass Transfer, 2010, 53(13-14): 2760-72.

[14] *Wang L, Yang T.,* Bifurcation and stability of forced convection in curved ducts of square cross-section. International Journal of Heat and Mass Transfer, 2004, 47(14-16): 2971-87.

[15] *Seader C E K A J D.,* Heat and mass transfer phenomena for viscous flow in curved circular tubes. Int J heat mass transfer, 1972.

[16] *G. Yang Z F D, M. A. Ebadian.,* Laminar forced convection in a helicoidal pipe with finite pitch. Int J Heat Mass Transfer, 1995.

[17] *Ghaedamini H, Lee P S, Teo C J.,* Developing forced convection in converging–diverging microchannels. International Journal of Heat and Mass Transfer, 2013, 65: 491-9.

[18] *Xie G, Liu J, Liu Y, et al.,* Comparative Study of Thermal Performance of Longitudinal and Transversal-Wavy Microchannel Heat Sinks for Electronic Cooling. Journal of Electronic Packaging, 2013, 135(2).

[19] *Xie G, Liu J, Zhang W, et al.,* Analysis of Flow and Thermal Performance of a Water-Cooled Transversal Wavy Microchannel Heat Sink for Chip Cooling. Journal of Electronic Packaging, 2012, 134(4).

[20] *Lin L, Zhao J, Lu G, et al.,* Heat transfer enhancement in microchannel heat sink by wavy channel with changing wavelength/amplitude. International Journal of Thermal Sciences, 2017, 118: 423-34.

[21] *Liang Gong K K.* Parametric numerical study of flow and heat transfer in microchannels with wavy walls. International Mechanical Engineering Congress & Exposition, 2010.

[22] *Manglik R M, Zhang J, Muley A.*, Low Reynolds number forced convection in three-dimensional wavy-plate-fin compact channels: fin density effects. International Journal of Heat and Mass Transfer, 2005, 48(8): 1439-49.

[23] *Li Y F, Xia G D, Ma D D, et al.,* Characteristics of laminar flow and heat transfer in microchannel heat sink with triangular cavities and rectangular ribs. International Journal of Heat and Mass Transfer, 2016, 98: 17-28.

[24] *Bejan A.* Entropy generation minimization: The new thermodynamics of finite-size devices and finite-time processes. Journal of Applied Physics, 1996, 79(3): 1191-218.

[25] *Liu C, Teng J-T, Chu J-C, et al.,* Experimental investigations on liquid flow and heat transfer in rectangular microchannel with longitudinal vortex generators. International Journal of Heat and Mass Transfer, 2011, 54(13-14): 3069-80.

[26] *R.L.Webb.,* Performance evolution criteria for use of enhanced heat transfer surfaces in heat exchanger design.pdf. Heat Mass Transfer, 1981: 12.